applied sciences

MDPI

Article

Study of the Load-Bearing Characteristics of Bolts under Asymmetric Freezing Conditions

Jie Dong [1,2,*], Xin Yan [1], Zhao-Qi Li [1], Yang Liu [1], Ying-Hao Zheng [1] and Kai Feng [1]

[1] College of Civil Engineering, Hebei University of Architecture, Zhangjiakou 075000, China
[2] Hebei Colleges Applied Technology Research Center of Green Building Materials and Building Reconstruction, Zhangjiakou 075000, China
* Correspondence: dongjie1003@hotmail.com

Abstract: To investigate the load-bearing characteristics of anchor rods under asymmetric freezing conditions such as those in cold regions and the effect of frost swelling, a model test device was developed using a controlled-temperature environmental box and a hydraulic actuator. Laboratorial pull-out model tests of anchor rods in soil layers were conducted at different moisture contents and freezing temperatures, the changes in anchor rod pull-out force before and after freezing were quantitatively described, load–displacement relationship curves were prepared, and the frost swelling displacement of anchor rods under asymmetric freezing conditions and the stress evolution of surrounding soil were observed and recorded. The shear strength of the anchor–soil interface increased with decreasing temperature, and the ultimate values of the pull-out force at 0, −3 and −7 °C were 4, 17.04 and 18.1 times greater than those at room temperature, respectively, for 10% water content. The pull-out force of the frozen anchor increased with increasing water content. The bolts were displaced by the freezing expansion force. Their lateral displacements at 0, −3 and −7 °C were 2.9, 3.2 and 3.5 mm, respectively, and their vertical displacements were 0.2, 3.5 and 4.3 mm, respectively, for 10% water content. The total displacement increased with increasing moisture content, and the maximum transverse displacements were 3.5, 3.65 and 3.8 mm for 10, 12 and 14% water contents, respectively, and 4.3, 5.1 and 5.5 mm in the vertical direction, respectively. The ultimate pull-out forces after freezing and thawing were 71, 68 and 52% of that before freezing for 10, 12 and 14% water, respectively.

Keywords: cold regions; bolt; asymmetric freezing

check for updates

Citation: Dong, J.; Yan, X.; Li, Z.-Q.; Liu, Y.; Zheng, Y.-H.; Feng, K. Study of the Load-Bearing Characteristics of Bolts under Asymmetric Freezing Conditions. *Appl. Sci.* **2023**, *13*, 3184. https://doi.org/10.3390/app13053184

Academic Editor: John D. Clayton

Received: 16 February 2023
Revised: 27 February 2023
Accepted: 28 February 2023
Published: 2 March 2023

Copyright: © 2023 by the authors. Licensee MDPI, Basel, Switzerland. This article is an open access article distributed under the terms and conditions of the Creative Commons Attribution (CC BY) license (https://creativecommons.org/licenses/by/4.0/).

1. Introduction

With the advantages of good mechanical properties, high reinforcement efficiency and good elasticity, anchor rod reinforcements are widely used in slope reinforcement, pit support, roadway excavation and other projects [1–3]. The stability and mechanical properties of loosely packed soils are enhanced by anchor reinforcement [4]. In some cold regions, the migration and formation of ice by water in soil at low temperature causes the soil around the anchor rod to enter a freeze state under the negative temperature load. The water in the soil solidifies into ice crystals that are immobile, expand in volume and fill the pores between the soil particles. The presence of ice crystals causes soil particles to crowd and changes the mechanical properties of soil.

Many scholars have studied the nature of permafrost. Some scholars evaluated the shear strength of frozen soil by direct shear tests [5–14]. Chen [15] developed model pile-testing equipment and used it to conduct several field freezing strength tests. The results showed that the freezing strength and residual freezing strength increased linearly with decreasing temperature. There is a limiting value of water content in frozen soil. When the water content in the soil is less than this value, the freezing strength and residual freezing strength increase with increasing water content and conversely decrease with increasing

water content. Li et al. [16] believed that the shear strength of permafrost increased linearly with decreasing temperature when the shear strength was shared by ice crystals and soil particles. Liu et al. [17] launched a large-scale direct shear test on permafrost soil and plotted shear stress–displacement curves. They considered that the damage process consisted of five parts: elastic deformation, plastic deformation, integral sliding, strain hardening and residual strength stabilization. The peak shear strength was linearly related to temperature and normal stress and nonlinearly related to the moisture content of the soil, and the moisture content had a more significant effect than temperature on the peak strength. The shear strength of frozen soil was related to the shear rate in the direct shear test. Xu et al. [18] considered the shear strength of permafrost to be influenced by the rate of damage, and the peak shear decreased with increasing shear rate. Andersland and Ladanyi [19] believed that the shear strength of permafrost was affected by the surrounding pressure of the soil. When the surrounding pressure was larger, the soil particles squeezed one other to increase soil compaction; however, the fracture of ice crystals was restricted, and the internal friction of the soil was enhanced. In contrast, Jones [20] believe that when the surrounding pressure was small, the water between soil particles produced a greater degree of expansion during freezing, which reduced the relative compaction of the soil and soil strength. Apparently, in the perennial permafrost region, there is strength anisotropy in the soil due to the formation of ice wedges according to Yang et al. [21].

The change in the underground environment temperature affects the load-bearing capacity of the soil mass and then changes the stress conditions of the underground infrastructure. Some engineering structures, such as underground pipe galleries, retaining walls and anchorage systems, are damaged [22]. The stress state and pull-out resistance of the anchor change due to the frost heaving force. Some scholars evaluate the bearing capacity of the frozen soil anchor through the shear strength of the interface between the bolt and frozen soil and analyse the influence of various factors on the load-bearing characteristics of the anchor and the safety of the anchoring project.

Aldaeef and Rayhani [23] proposed the “m” coefficient to evaluate the roughness of the interfaces of anchors in frozen sand. The shear strength of the interface was related to the cohesion and friction of the frozen soil. The peak strength of the sample increased with decreasing exposure temperature and increasing normal stress change rate, and the “m” coefficient decreased with decreasing temperature.

In the available research on frozen soil [24–28], some scholars studied the effects of freezing temperature, soil confining pressure, dry density and water content on the interfaces between frozen soil and structures. The results showed that the shear strength of the anchor–soil interface increased linearly with decreasing temperature and increasing normal stress. When the temperature rose, the anchorage bearing capacity was obviously lost. The pull-out resistance of the frozen soil anchor was several times or even more than ten times that of unfrozen soil. In anchoring projects, the axial force of the anchor in the initial freezing state significantly increased [29,30]. When the temperature rose, the axial force decreased rapidly when the frozen soil melted, and it was difficult for the axial strength to recover to the level before freezing. Additionally, the anchoring force on soil after frozen soil thawed decreased year by year.

Johnston [31] and Aldaeef [32] considered that every time the soil freezes and thaws, the underground structure inevitably produces relative dislocation with the surrounding soil, the frost heaving force has a creep effect on the underground structure, and its bearing capacity changes with creep displacement. The displacement of the structural damage position of the slope anchor in the seasonal freezing area occurs frequently due to freezing expansion and thawing settlement [33–35]. Damage to the anchor bolt by the pull-out force is caused by freezing and thawing cycles. Zhang et al. [36] considered that the ultimate pull-out bearing capacity of the bolt decreased with increasing number of freeze–thaw cycles, and freeze–thaw damage was relatively rapid. In the past, research on anchor bolts in frozen soil focused on the relationship between freezing parameters and shear strength but did not pay enough attention to the freezing method, and most studies adopted one-

way freezing. However, the transmission direction of a negative temperature load in nature often has a certain angle with respect to the structure. For example, in slope engineering in cold regions, the frozen front is constantly diffusing inwards from the slope surface, and the temperature gradient line intersects the anchor rod in a nonvertical direction. This leads to the anchor rod entering an asymmetric freezing state, and the two sides bear asymmetric frost heaving forces, as shown in Figure 1. In this study, the load-bearing characteristics of anchors under asymmetric freezing conditions were studied by indoor pull-out tests of frozen soil bolts.

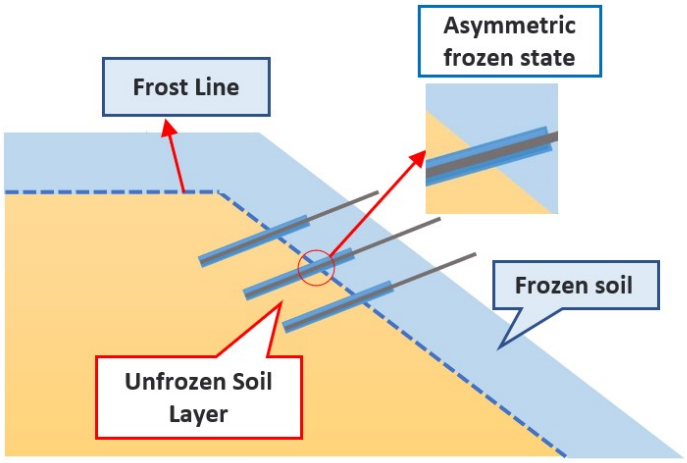


Figure 1. Schematic diagram of asymmetric freezing of a bolt.

2. Methods and Material Studied

2.1. Material Parameters and Anchor Preparation

The test filler was fine sand with different moisture contents, and the relationship between the peak shear force and vertical stress of the damaged interface of the soil sample was obtained by direct shear tests. The sand comes from Wushen County, Inner Mongolia, China. The Cullen–Moore criterion was used to analyse the damaged interface to determine the friction angle and soil cohesion within the soil, as shown in Table 1.

Table 1. Sand parameters.

w/%	c/kPa	φ/°
10	12	24.2
12	10.5	24.0
14	9.6	23.7

According to the table, the internal cohesion of wind-deposited sand decreased continuously by 20% when the water content increased from 10 to 14%, while the internal friction angle changed very little.

The prefabricated anchor rod selected for this test was made of M8 threaded wire rod and cement mortar, the thread material was steel with good corrosion resistance, and the cement was ordinary silicate cement with strength grade PO. 42.5. The cement was poured and initially settled in a custom mould. The main body of the mould was an acrylic hollow tube, 300 mm long, with inner diameters 30, 35 and 40 mm and wall thickness 2 mm. For later demoulding, the mould was cut along the longitudinal axis and coated with machine oil before cement was cast. After pouring, the anchor was left to stand for 24 h, and the anchor was demoulded and maintained after the initial setting. The ratio of cement mortar was ordinary silicate cement:standard sand:water = 1:1:0.43. Finished anchors are shown in Figure 2. The compressive strength test shows that the mortar has a compressive strength of 21 MPa.



Figure 2. Bolt models.

2.2. Testing Equipment

To study the effect of low-temperature environments on the anchorage force, a model test device was designed based on a controlled-temperature environment box and a hydraulic actuator. The device consisted of a movable reaction frame, actuator with hydraulic fixture, actuator control and acquisition system, servo oil source power system, refrigeration system, and a controlled-temperature environment box. The schematic diagram is shown in Figure 3.

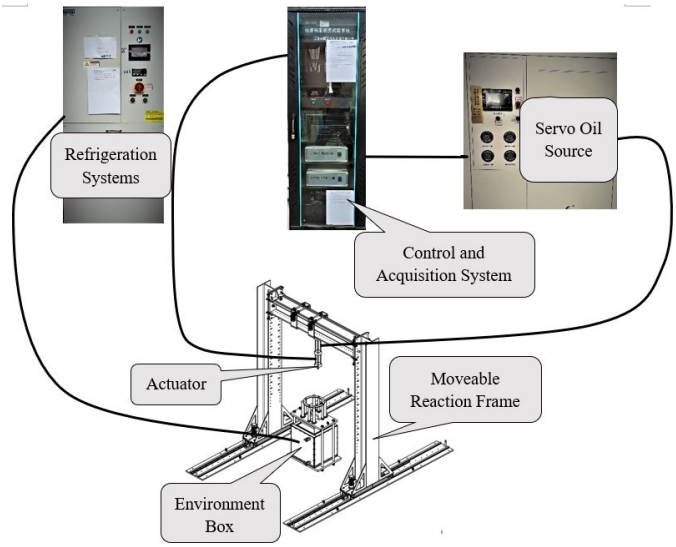


Figure 3. Schematic diagram of the test equipment.

In this test, an MXX-600 multifunction model test box was used to mainly undertake the role of holding test materials and providing a negative temperature environment. The main body was a hollow cube with four side walls, and it was welded steel. The outer diameter was 830 mm × 83 0 mm × 1000 mm (L × W × H), the thickness of the side walls was 115 mm, and the inner diameter of the model box was 600 mm × 600 mm × 980 mm (L × W × H). The surrounding side walls were internally connected hollow structures, where antifreeze circulated when a negative temperature load was applied.

In this test, the asymmetric freezing mode was achieved by placing insulation boards of different heights inside the box, with 600 mm high insulation boards on three sides and 300 mm high insulation boards on one side; the unshaded area was the freezing area, which was 300 mm × 300 mm. The top view of the model box and the negative temperature load propagation schematic are shown in Figures 4 and 5, respectively. The test equipment was manufactured by JiLin Guanteng Automation Technology Co., Ltd. (Changchun, China).

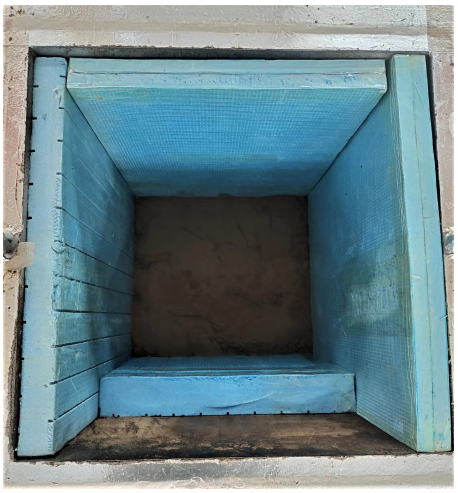


Figure 4. Top view of the model box.

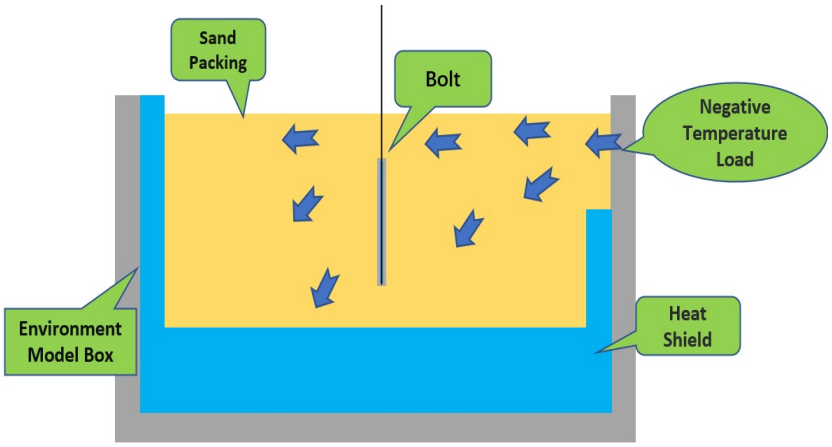


Figure 5. Schematic diagram of negative temperature load transfer.

2.3. Testing Process

In this study, we considered the influence of the anchorage diameter, moisture content and ambient temperature and evaluate combinations of parameters and variables. The test was mainly divided into three components: the first component was the static pulling test in laboratorial temperature environment; the second was the static pulling test under asymmetric freezing with different negative temperature conditions; and the third was the static pulling test after freeze–thaw damage. The freeze–thaw process was freezing to −7 °C and then thawing to room temperature. The test conditions are shown in the following Table 2.

The prefabricated anchors were fixed by anchor aligners, and the layered filling method was used to fill the environmental model with soil and to lay earth pressure boxes and temperature sensors at predetermined monitoring locations. The soil pressure box was vertically laid in the horizontal direction with sensors from No. 1 to No. 5 to collect the horizontal stress. No. 1 was 50 mm from the right wall, and the distance from pressure box No. 2 was 100 mm; No. 3 was placed near the anchor, and Nos. 4 and 5 were symmetrically arranged with respect to Nos. 2 and 1. Longitudinally from top to bottom, Nos. 6 to 9 were transversely laid to collect the vertical freeze pull-out force. No. 9 was placed 150 mm above the bottom plate, No. 6 was located 150 mm below the soil surface, and the rest of the spacings were 100 mm.

The temperature sensors were laid in a horizontal × vertical direction of 5 × 4. The negative temperature load was applied after the filling was completed. The collection of earth pressure and temperature sensor data was completed during the freezing process;

pulling was performed when freezing to the corresponding temperature. The filling process is shown in Figure 6.

Table 2. Test conditions.

Bolt Diameter/mm	Number	Moisture Content/%	Temperature/°C	Anchorage Volume/m^3
30	1	10	23	0.021
35	2	10	23	0.029
40	3	10	23	0.038
30	4	12	23	0.021
35	5	12	23	0.029
40	6	12	23	0.038
30	7	14	23	0.021
35	8	14	23	0.029
40	9	14	23	0.038
30	10	10	0	0.021
30	11	12	0	0.021
30	12	14	0	0.021
30	13	10	−3	0.021
30	14	12	−3	0.021
30	15	14	−3	0.021
30	16	10	−7	0.021
30	17	12	−7	0.021
30	18	14	−7	0.021
30	19	10	Melted	0.021
30	20	12	Melted	0.021
30	21	14	Melted	0.021



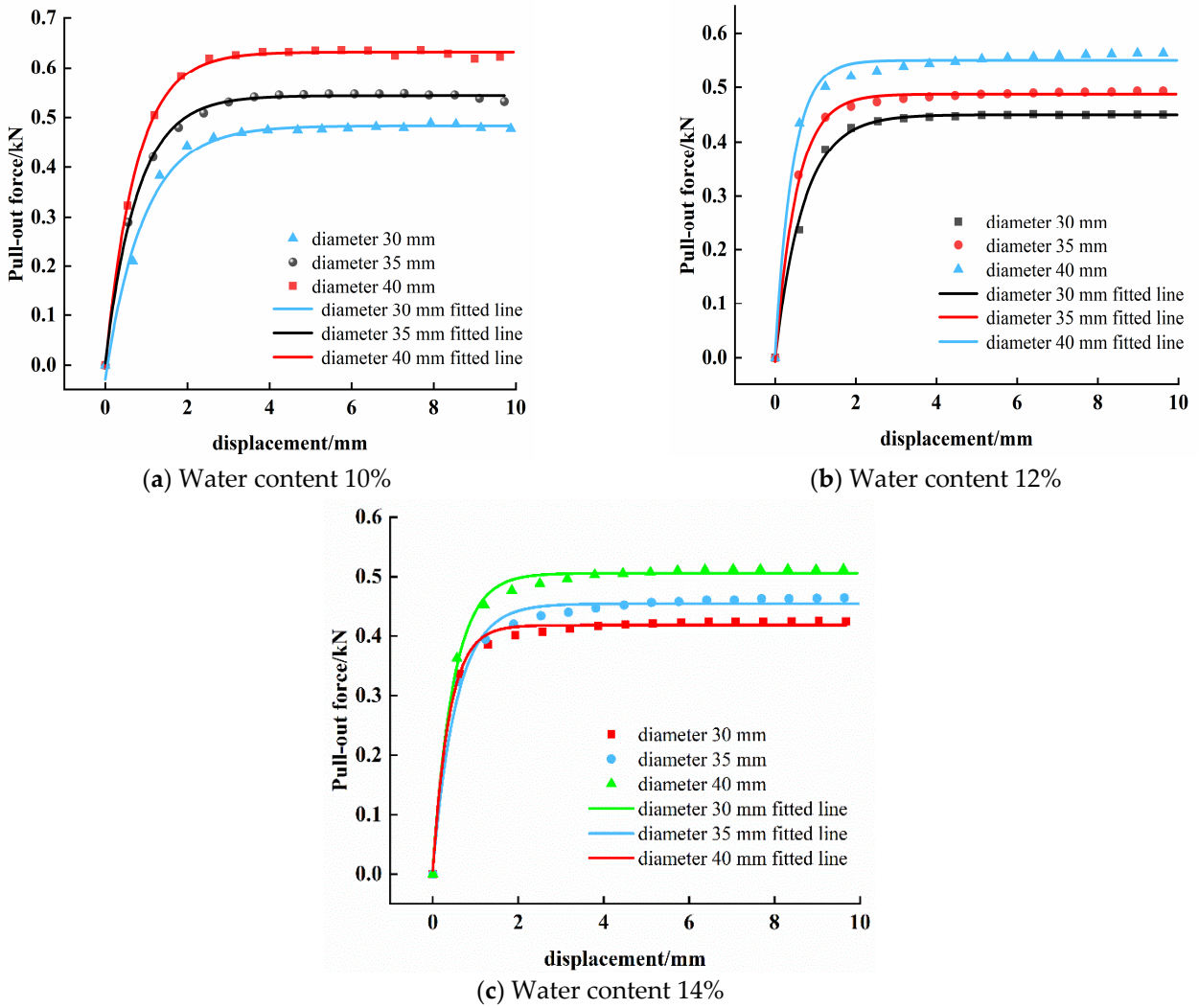
Figure 6. Filling process.

3. Results and Analyses

3.1. Analysis of the Results of the Indoor Pulling Test of the Bolt

3.1.1. Influence of the Anchor Size on the Ultimate Pull-Out Force

To further study the influence of the anchorage size on the bearing characteristics of uplift resistance, anchors with diameters of 30, 35 and 40 mm were selected as the comparison conditions, and soils with moisture contents of 10, 12 and 14% were combined for indoor pulling tests. The results are shown in Figure 7.



(**a**) Water content 10% (**b**) Water content 12%

(**c**) Water content 14%

Figure 7. Load-bearing capacity-displacement curves for bolts of different diameters.

For force-displacement data, a variety of functions were tried to fit, and the exponential function was found to be more appropriate. The curves of load-bearing capacity of the bolt vs. axial displacement of the bolt for different anchor sizes are shown in Figure 7. According to the analysis:

(1) The pull-out force of the anchor rod increased with increasing axial displacement, and the pull-out damage process could be divided into three stages: "fast growth", "slow growth" and "constant growth". Phase 1: The pull-out resistance increased rapidly with increasing pull-out displacement between 0 and 1 mm. Taking the water content of 10% as an example, the pull-out resistance of the 30 mm diameter anchor rod increased by 0.4 kN during this stage, while for bolts with 35 and 40 mm diameters, the pull-out force increased by 0.43 kN and 0.52 kN, respectively, accounting for 84% of the respective ultimate pull-out resistance, and the force–displacement curve

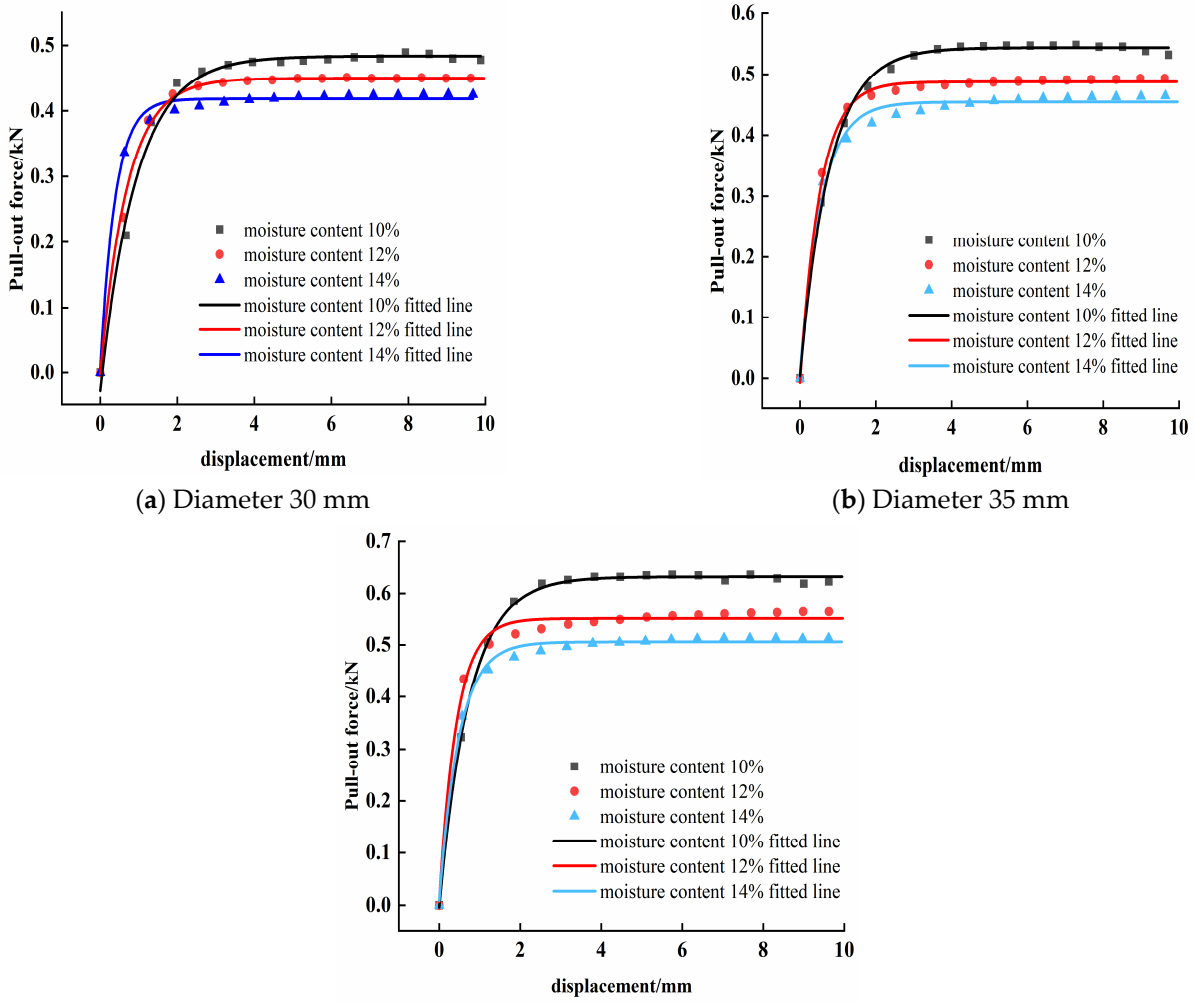
maintained a linear increase. Phase 2: The pull-out force increased slowly with increasing displacement from 1 to 3 mm, and the growth rate decreased continuously. The pull-out force basically reached the ultimate pull-out value at this stage. Phase 3: the pull-out force remained constant with increasing pull-out displacement from 3 to 10 mm, and the anchor pull-out force reached its limit and stabilized. The anchor formed a sliding state at the anchor–soil interface, and the pull-out force was provided entirely by the frictional force at the shear interface, at which time the anchor system could be considered to have failed. However, since the anchor rod was not completely pulled out, the anchor force maintained the peak state for a long time without decay.

(2) The ultimate pull-out resistance of the anchor was influenced by the diameter of the anchor. The ultimate pull-out values of anchors with diameters of 30, 35 and 40 mm at 10% moisture content were 0.49, 0.54 and 0.64 kN, respectively. The pull-out resistance increased with increasing diameter, and the pull-out resistances of 35 and 40 mm diameters were 1.102 and 1.306 times that of anchors with 30 mm diameter, respectively. The ultimate pull-out resistances of anchors with diameters of 30, 35 and 40 mm were 0.45, 0.49 and 0.56 kN, respectively, at 12% moisture content, and the pull-out resistances of those with 35 and 40 mm diameters were 1.089 and 1.254 times that of 30 mm anchors, respectively. The ultimate pull-out resistance values of anchors with diameters of 30, 35 and 40 mm were 0.426, 0.464 and 0.513 kN, respectively, at a moisture content of 14%. The pull-out resistances for diameters of 35 and 40 mm were 1.091 and 1.248 times that of 30 mm anchors, respectively. An appropriate increase in the diameter of the anchor will have a good effect on increasing the anchorage force.

(3) The displacement corresponding to the ultimate pull-out force was basically the same for anchors with the three diameters and the same moisture content, i.e., the inflection point where the force–displacement curve tended to be flat remained the same. The displacement at the ultimate force for the 10% water content condition was 2.67 mm, while the displacements at the ultimate force for 12% and 14% water contents were 1.91 and 1.87 mm, respectively. This was because the soil properties determined the shear strength of the anchor–soil interface. Increasing the anchor diameter made the anchor-soil interface, i.e., the area providing friction, larger, and then the peak anchor force increased, but there was no change in the shear stress state of the anchored soil. The shear strength of any soil unit on the contact surface did not change due to the anchor size, so the displacement of specimens with different anchor diameters was generally the same when the limiting state was reached.

3.1.2. Influence of Moisture Content on Ultimate Pull-Out Resistance

Figure 8 shows that the ultimate pull-out resistance of anchors of the same anchorage diameter decreased with increasing water content of the soil. Taking 30 mm diameter anchors as an example, the ultimate pull-out resistances for 10, 12 and 14% water contents were 0.49, 0.451 and 0.4256 kN, and the increase in water content from 10 to 12 and 14% reduced the anchor pull-out resistance by 0.039 and 0.064 kN, respectively, reductions of 7.96 and 13.1%, respectively. The increase in water content from 12 to 14% reduced the ultimate pull-out resistance by 0.0254 kN (5.63%). For 35 mm diameter anchors, the anchor pull-out resistance was reduced by 0.05 and 0.076 kN when the water content was increased from 10 to 12 and 14%, respectively, reductions of 9.26% and 14.1%. When the water content was increased from 12 to 14%, the ultimate value of the pull-out resistance was reduced by 0.0256 kN, a reduction of 5.22%. For increases in the moisture content of 40 mm diameter anchors from 10 to 12 and 14%, the anchor pull-out force was reduced by 0.0754 and 0.127 kN, respectively, with reductions of 11.78% and 19.84%. The water content was increased from 12 to 14%, and the ultimate value of the pull-out resistance was reduced by 0.051 kN, a reduction of 9.1%.



(**a**) Diameter 30 mm (**b**) Diameter 35 mm

(**c**) Diameter 40 mm

Figure 8. Uplift bearing capacity–displacement curves of anchors with different water contents.

Figure 8 shows that the displacement corresponding to the ultimate pull-out resistance reached by the same anchor decreased with increasing water content. Taking the 35 mm diameter anchor as an example, the displacements at 10, 12 and 14% of the ultimate anchorage force were 1.7, 2.2 and 2.9 mm, respectively. For each working condition, the 14% specimen was the first to reach the limit, followed by 12% and finally, 10%. This behaviour can be explained by the increase in water content that weakened the shear strength of the anchoring interface. When pulled by the same displacement, the soil with higher moisture content had less shear potential, and the contact interface was less capable of continuously exerting shear action, and thus, damage occurred earlier.

When the water content increased, a large amount of freely movable pore water was present between the soil particles, the mobility of the soil particles was enhanced, the stability became poor, and the shear strength of the unit soil at the anchor–soil interface decreased. In turn, the smoothness of the contact surface was enhanced, and the ultimate anchorage force was reduced. When the water content of the anchored soil rises due to rainfall and other factors, the anchoring capacity of the anchor decays to different degrees.

3.2. Study on the Bearing Characteristics of Bolts in a Cold Environment

Frost heaving occurs when soil drops to a negative temperature due to environmental influences, and the properties of the soil change dramatically. Under these conditions, the soil is referred to as frozen soil, and it is mainly composed of soil particles, ice crystals and trace amounts of water. Soil freezing is an expansion process, and the underground

structure in cold areas is inevitably affected by the frost heave force. Thus, frost heave is an important factor affecting the safety of engineered structures in cold regions.

Figure 9 shows the temperature distribution clouds of the soil in the model box at different times under negative temperature loading. Figure 9 shows that with increasing freezing time, the negative temperature load was continuously applied from the cold source to the soil mass, the temperature of each monitoring point continued to decrease, the frozen area continued to spread from the cold source to the inside of the soil mass, the freezing depth continued to deepen, and the frozen soil area continued to expand.

At the beginning of freezing, the soil at the cold source was the first to drop to a negative temperature, and there was only one layer of frozen soil at this time. As the negative temperature load advanced to the left, when the freezing time was 5 h, the soil near the cold source was in the approximate shape of a rectangle, and the freezing front was vertical and spread in a uniform manner.

When frozen for 10 h, approximately one-quarter of the whole area had a negative temperature, the shape of the frozen area was triangular, and the diffusion mode propagated from a straight line to an arc. At this time, the soil mass on the upper right of the bolt in the centre of the model box entered the freezing stage, and the upper part of the bolt was subjected to the horizontal frost heaving force and upward pulling force from right to left. Under the action of the frost heave force, the horizontal displacement of the anchor began to occur, and the vertical displacement did not change.

When frozen for 15 h, approximately one-third of the whole area entered a negative temperature state, and the negative temperature spread out in an arc. At this time, the soil around the upper half of the bolt basically entered a negative temperature state, and its right side was frozen, while the left side had just frozen. The horizontal frost heave force on the rod body was still directed to the left, and the force on the shaft gradually decreased from top to bottom. At this time, the upper part of the bolt was subjected to the vertical upward freezing pulling force, the lower part of the soil did not undergo freeze heave, and downward friction force was applied to the bolt. At this time, the freezing pulling force and the friction force were in opposite directions, and the vertical displacement was relatively small.

After freezing for 20 h, approximately half of the whole sample entered a negative temperature state, and the soil around the bolt was basically frozen. The freezing scale of the soil on the left side of the upper half of the bolt continued to develop, and the horizontal frost heave force to the right gradually occurred, which resisted the frost heave force to the left of the frozen soil on the right, and the increment of the left displacement of the bolt began to slow. The lower half of the bolt entered the freezing stage, the longitudinal freezing force ran through the entire bolt, and the overall vertical displacement began to occur.

After freezing for 30 h, almost all the soil in the model box entered the negative temperature state, the negative temperature load continued to propagate to the left wall and floor of the model box, the frost heave of the soil on the left side of the anchor continued to expand, the frost heave force was continuously enhanced but did not reach the right level, and the overall horizontal resultant force direction was still to the left. At this time, the lateral displacement of the bolt gradually slowed, and the vertical displacement continued to develop.

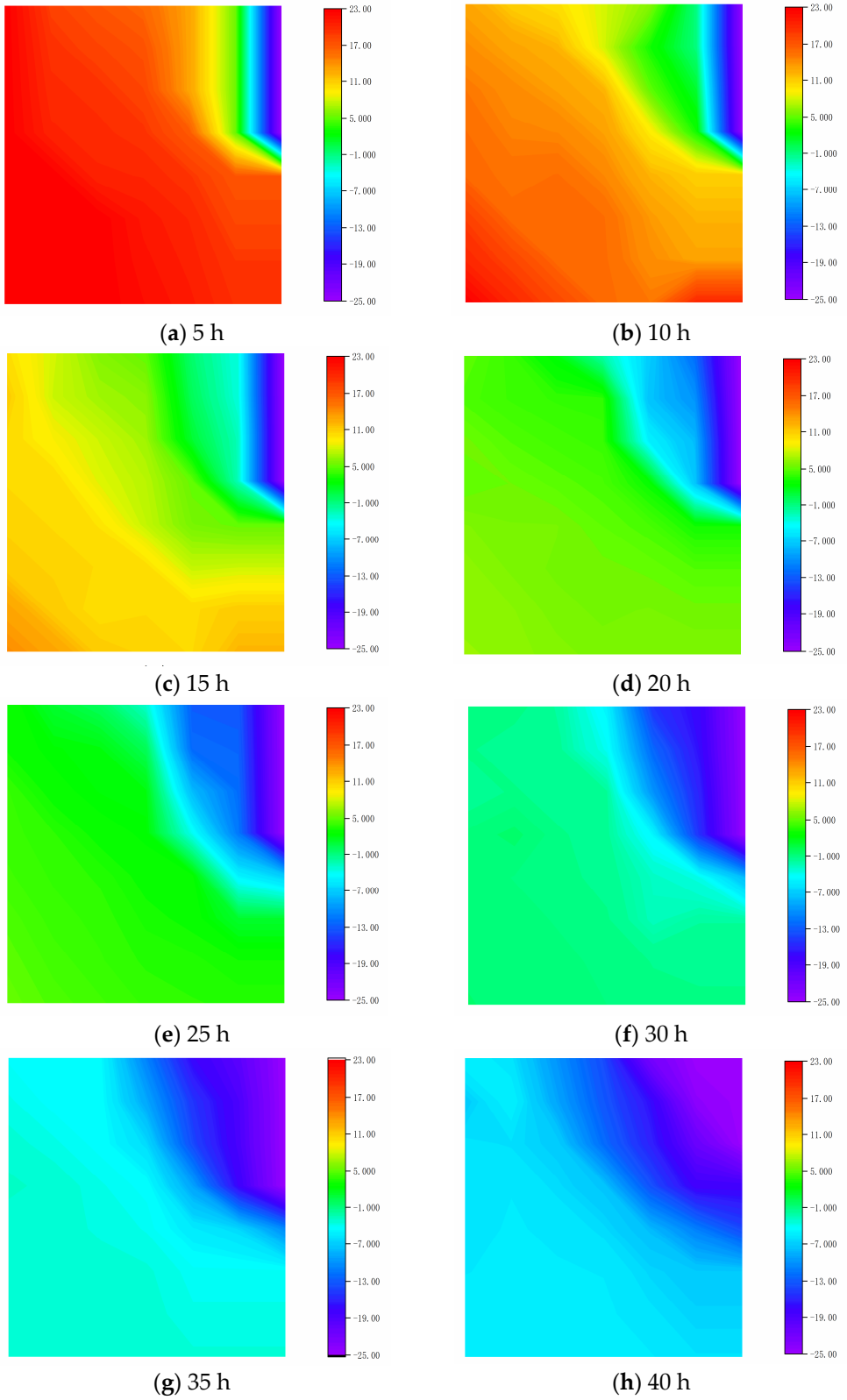


Figure 9. Cloud maps of soil temperature at different freezing times.

3.2.1. Effect of Frost Heave on Anchored Soil Stress

To explore the internal stress changes in frozen soil, a microscale earth pressure box was used to collect stress of soil at key positions around the bolt. The collected data are shown in Figures 10 and 11, where the abscissa is the temperature at the centre of the bolt.

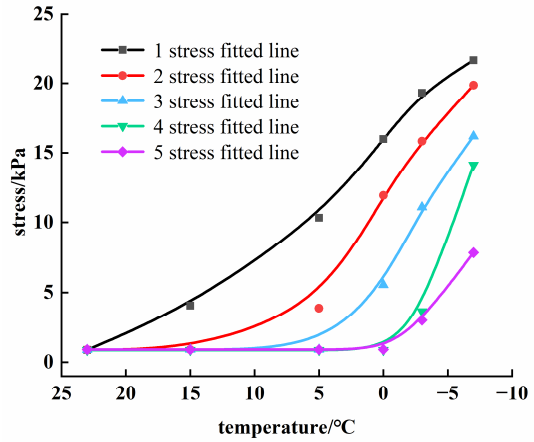


Figure 10. Horizontal stress curve.

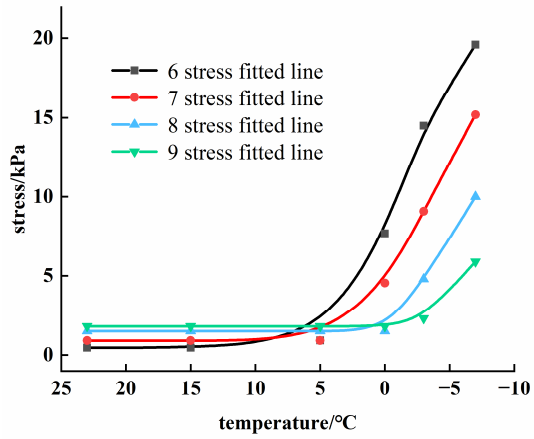


Figure 11. Vertical stress curve.

According to the analysis of Figure 10, the horizontal frost heave force at each monitoring point increased to different degrees with decreasing temperature. Because monitoring point No. 1 was first affected by the negative temperature load, it entered the freezing state earlier than the other monitoring points, and the horizontal stress increased first. Because monitoring point No. 5 was farthest from the cold source, it had the latest contact with the negative temperature load and remained unfrozen for a long time; the horizontal stress developed last.

When the core temperature of the bolt was reduced to 0 °C, the surface of the shaft was subjected to a frost heave confining pressure of 5.54 kPa, and when it was reduced to −3 °C and −7 °C, the pressure around the rod increased to 11.09 kPa and 162 kPa, increases of 55.5 kPa (100.1%) and 106.6 kPa (192.4%), respectively.

Because soil at different locations entered the frozen state at different times, the retaining pressure of the bolt was asymmetrical. When the temperature at the centre of the bolt was 5 °C, the soil around the rod had not yet frozen, but the soil to the right had undergone frost heaving, and the frost heaving force reached 3.89 kPa. The soil mass was compacted under the action of horizontal force, and the horizontal stress slightly increased. It was difficult for the unfrozen weak soil on the left side of the bolt to provide horizontal support, and thus, the bolt was displaced to the left by the asymmetric force.

When the temperature dropped to 0 °C, the stress difference between the two sides was 11.05 kPa, then the compressive strength of the soil on the left side of the bolt gradually increased as it entered the frozen state. The stress difference down to −3 °C was 12.18 kPa, while the difference was 5.74 kPa at −7 °C. Under the condition of lateral freezing, the bolt would be in an asymmetric confining pressure state for a long time.

Figure 11 shows that the vertical frost heaving force of each monitoring point increases with decreasing temperature. The upper soil mass has already entered the freezing state before the centre dropped to the negative temperature and had a vertical frost pull-out force. When the centre temperature was 0 °C, the freezing stresses at 50 and 150 mm above the centre, i.e., monitoring points Nos. 7 and 6, reached 4.54 and 7.7 kPa, respectively, while the soil below did not freeze and was only self-weight stress. When the temperature dropped to −7 °C, the stresses at the monitoring points from top to bottom, i.e., Nos. 6, 7, 8 and 9, were 19.6, 15.2, 10.0 and 5.9 kPa, with increases of 154.5, 234.8, 566.7 and 227.8%, respectively, compared with 0 °C. The vertical stress growth in the soil around the anchor rod was in the form of "diffusion" from top to bottom.

3.2.2. Influence of Frost Heaving on Bolt Displacement

The horizontal frost heaving force and the longitudinal frost pulling force generated during the soil freezing process affect the spatial position of the anchor bolt. Under different freezing temperatures, the horizontal and vertical displacements of the anchor bolt are shown in Figures 12 and 13. The temperature was that at the anchor bolt centre.

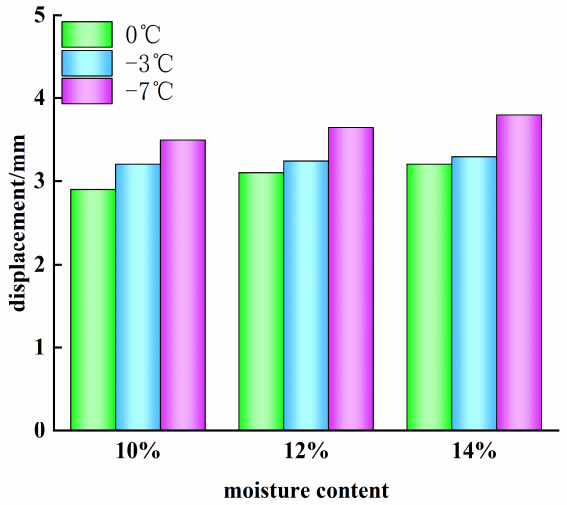


Figure 12. Horizontal displacement of the anchor rod at different temperatures.

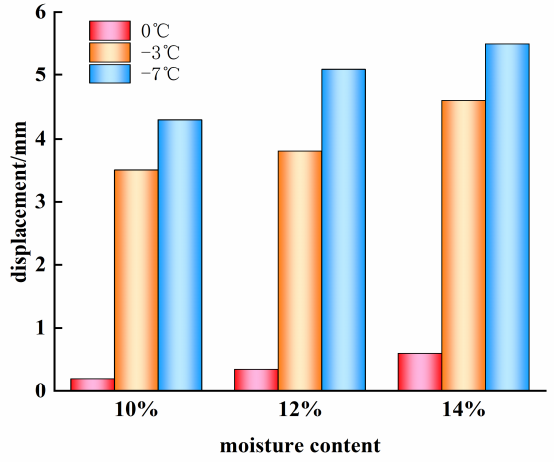


Figure 13. Vertical displacement of bolts at different temperatures.

The analysis of Figure 12 shows that the horizontal displacement of the anchor rod under the same water content condition increased to varying degrees with decreasing temperature. For the same freezing temperature, the frost heave displacement increased slightly with increasing water content. For every 2% increase in water content, the displacement increased by from 3% to 7%. For the sample with 10% water content, when the

soil mass dropped from room temperature to 0 °C, the anchor rod had a large horizontal displacement of 0.29 mm. When the temperature dropped to −3 °C and −7 °C, the horizontal displacement increased by 0.03 and 0.06 mm, which were 10.3 and 20.6% of the displacement when the temperature dropped to 0 °C, respectively.

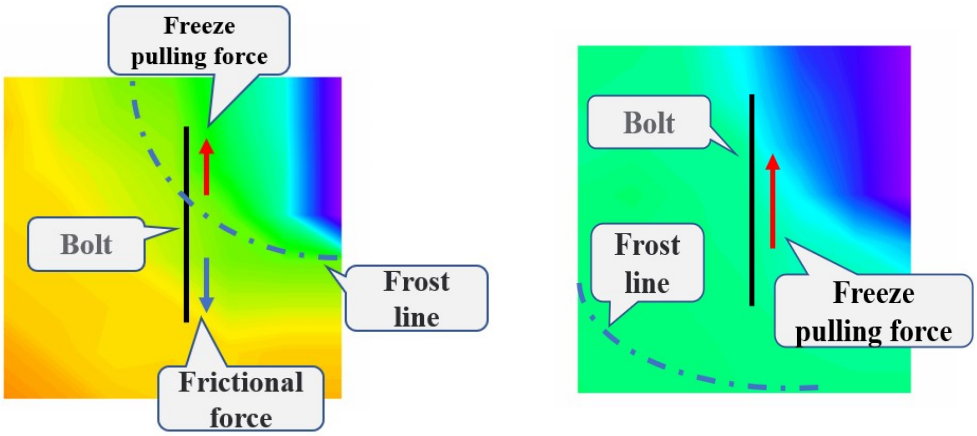
The reason for this behaviour can be explained as follows. The soil mass on the right side of the rod body froze and further expanded before the temperature at the centre of the bolt dropped to zero. During this process, water continuously migrated to the right and condensed, the strength of the soil on the right side constantly improved, and the frost heaving force on the rod was exerted to the left. As the soil on the left side of the anchor had not yet entered frozen, it was softer than the frozen soil and had poor resistance to the load on the right side, and the anchor was displaced under the action of the horizontal thrust.

During the process from 0 to −3 °C, the strength of the soil mass on the left side of the anchor bar gradually increased as it entered the negative temperature state. The soil gradually developed the ability to resist the load on the right side and produce the frost heaving force on the anchor bar to the right, but the force on the left side was still smaller than the horizontal resultant force on the right side, and the overall direction was still to the left. Although the soil stress values on both sides still maintained a certain gap, the left side had a certain strength after freezing, and the soil changed from soft to hard. Therefore, the displacement change at this stage kept increasing, but the increase was greatly reduced. During the process from 3 to –7 °C, the frozen soil on both sides of the bolt simultaneously developed to reach a lower temperature, the frost heaving effect continued to have an effect, and the displacement was similar to that during the previous stage and underwent a small amount of development.

Due to the free interface above the model, the bolt was vertically dislocated with the free expansion of the frozen soil in the vertical direction. The analysis of Figure 13 shows that the vertical displacement of the bolt increased with increasing moisture content and decreasing freezing temperature, and the increase was related to the longitudinal distribution of the gradient of freezing temperature. The vertical displacement of the bolt under the same freezing temperature conditions increased with increasing moisture content.

Taking the working condition of 10% moisture content as an example, the freezing displacement value of the rod body was 0.2 mm when the core temperature of the bolt was reduced from room temperature to 0 °C. When the temperature dropped to −3 °C, the displacement increased by 3.2 mm, a 15-fold increase. From −3 to −7 °C, the displacement continued to increase by 0.8 mm. The longitudinal frost heave effect was most significant when the temperature of the centre of the bolt was reduced from 0 to −3 °C.

The reason for this behaviour can be analysed as follows. When the centre of the rod body was 0 °C, only the upper part of the bolt produced a vertical upward freezing pulling force, while the lower part of the unfrozen soil produced vertical and downward friction on the anchor rod, and the mutual resistance to displacement of the two surfaces did not increase significantly. The freezing line expanded from top to bottom as the temperature decreased, and it gradually extended to the lower edge of the rod body when the central temperature of the bolt dropped to −3 °C. At this time, the bolt was basically surrounded by frozen soil, and the frost heave force ran through the whole bolt while the friction against it decreased to zero. Therefore, the displacement developed more rapidly in this process and was a significant effect of freezing. Figure 14 shows the force diagram of the bolt, and the background of the figure is the temperature distribution cloud at this time.

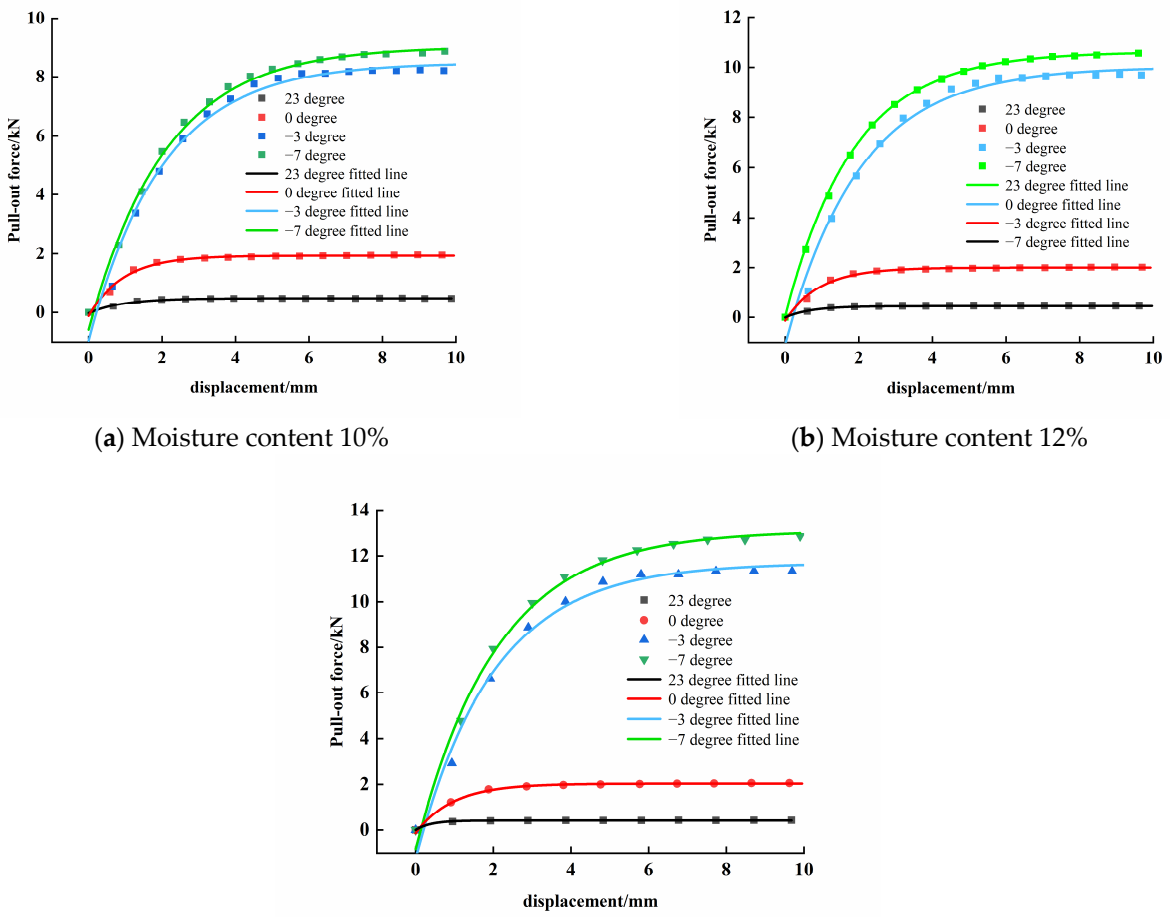


(**a**) 0 °C (**b**) −3 °C

Figure 14. Schematic diagram of the bolt force under different temperature gradients.

3.2.3. Effects of Freezing and Swelling on the Extraction Force

The shear strength of the anchor–soil interface was enhanced by the increase in the surrounding pressure on the anchor rod after the soil froze, and the anchor rod pull-out force vs. axial displacement under different temperature conditions is shown in Figure 15.



(**a**) Moisture content 10% (**b**) Moisture content 12%

(**c**) Moisture content 14%

Figure 15. Pull-out force vs. displacement at different temperatures.

Analysis of Figure 15 yielded the following insights:

(1) The ultimate value of the anchor pull-out force at each water content condition increased with decreasing temperature. Taking the moisture content of 10% as an example, the ultimate pull-out force at room temperature was 0.49 kN, and the ultimate values of the pull-out force under freezing to 0, −3 and −7 °C were 1.96, 8.35 and 8.87 kN, which were 4, 17.04 and 18.1 times higher than those at room temperature, respectively. This behaviour can be explained as follows: the soil entered a frozen state under the negative temperature load, the water in the soil froze and expanded in situ, the condensed ice crystals filled the gaps between the soil particles and tightly squeezed them, the compactness of the soil increased, the normal stress on the anchor rod body increased, the shear strength of the anchorage interface was enhanced, and the load-bearing capacity of the anchor rod in frozen soil could reach more than ten times that in unfrozen conditions.

(2) When the centre of the anchor was at 0 °C, the surrounding soil was about to freeze, and some of the unfrozen water still maintained a small amount of mobility between the soil particles. The liquid phase in the soil was in an ice–water mixture, and the pull-out resistance underwent a small increase due to partial freezing of water. At the stage from 0 to −3 °C, the soil moisture around the rod basically entered the frozen state, the interstices of soil particles were filled with ice crystals, and the pull-out resistance and soil strength grew rapidly. At the stage from −3 to −7 °C, only a small amount of water in the soil had not frozen, the pull-out force growth potential was small, and thus, the limiting value of the pull-out force at this stage had only a small increase compared with the former.

(3) At the same temperature, the limiting value of the pull-out force increased with increasing water content. Taking the working condition of −3 °C as an example, the limiting values of the pull-out forces of 10, 12 and 14% water content were 8.25, 9.74 and 11.39 kN, respectively. Compared with the working conditions of 10, 12 and 14% water content, the pull-out force increased by 1.49 and 3.14 kN, respectively, with increases of 18.06% and 38.06%, respectively. With the increase in soil moisture content, there was more liquid water between particles. The freezing expansion increased with increasing water content. The greater the degree of compaction of soil particles and ice crystals was, the greater the ability of the anchor to withstand confining pressure and shear resistance.

(4) The stress displacement curve of the frozen soil anchor rod could also be divided into three stages: “rapid growth”, “slow growth” and “maintain the same”. Unlike the normal temperature condition, the stress growth stage of the freezing condition was longer before entering the failure stage. In the first stage, the drawing force increased rapidly with displacement, and the stress displacement increased linearly. In the second stage, the slope of the curve was gradually attenuated from 2 to 7 mm, and the relationship between the drawing force and the displacement was nonlinear. In the third stage, the curve entered the horizontal development stage between 7 and 8 mm, at which time the pull-out force basically reached the limit state. The pull-out force did not change with increasing displacement, and thus, the anchoring force was considered invalid.

The extremes of the pull-out force of the frozen bolt at different water content show an exponential growth pattern with the decrease of freezing temperature (as shown in Figure 16). The peak pull-out force grows faster in the early stage, then slows down and tends to a stable point in the later stage. This is due to the fact that as the freezing temperature decreases, the water migration and ice formation process is gradually completed, and the pull-out resistance has no more growth potential.

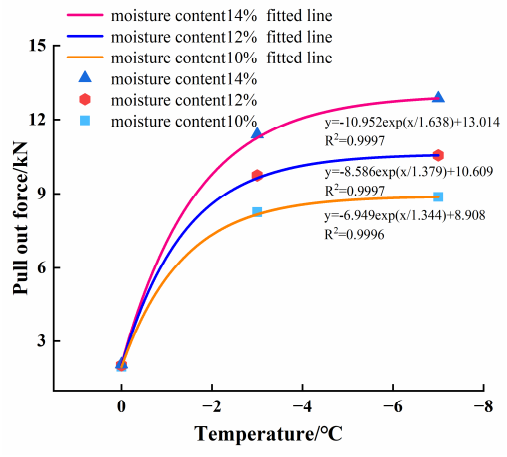


Figure 16. Extremes of pull-out force versus freezing temperature curve.

3.2.4. Influence of Melting on the Ultimate Pull-out Force

The relationship between the melting and sinking action and the anchor pull-out force is shown in Figure 17, and the freezing temperature was selected as −7 °C.

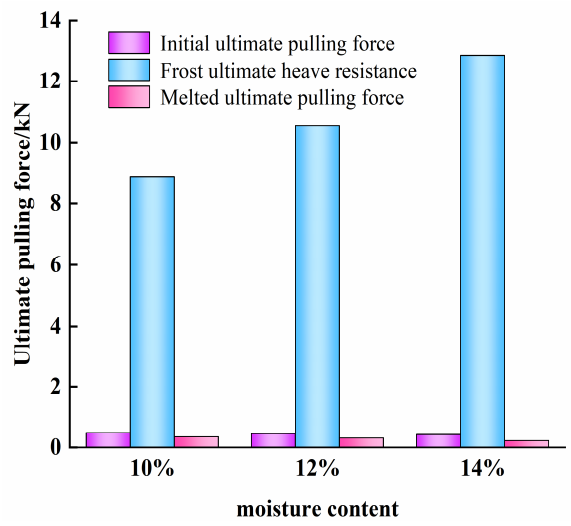


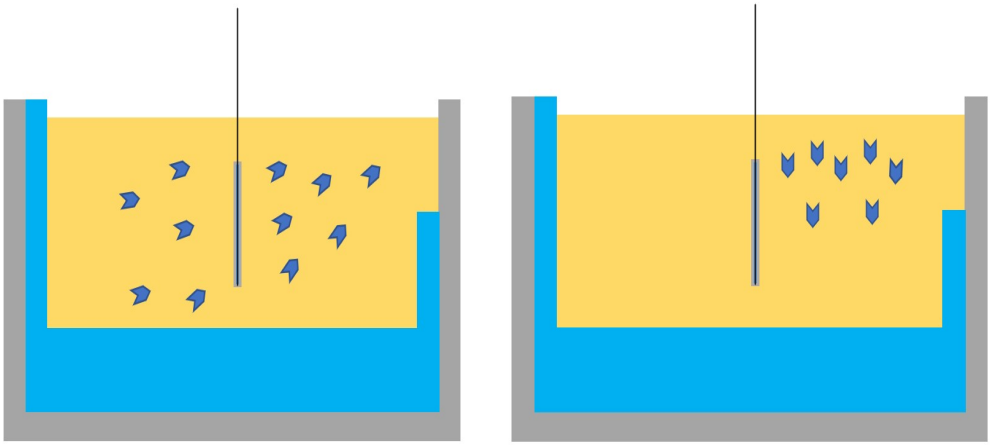
Figure 17. The relationship between the melting action and the ultimate pull-out force of bolts.

Analysis of Figure 17 shows that:

(1) The ultimate pull-out force of soil in the frozen state was the largest, and that of soil in the molten state was the smallest, under the same water content working condition. The pull-out force under frozen conditions was much greater than that before freezing and after thawing, the freezing and thawing effect greatly weakened the pull-out force of frozen soil, and the pull-out force after thawing was less than that before freezing. Taking the moisture content of 10% as an example, the pull-out force in the frozen state and after thawing was 16.8 times and 0.71 times that before freezing. When the soil around the anchor solid entered the frozen state, the water in the soil condensed into larger ice crystals and migrated continuously in the direction of the cold source. However, freezing and expansion increased the spacing of soil particles and was irreversible. The frozen soil melted when the temperature rose, and the melting sequence was from top to bottom; a large amount of liquid phase water appeared at the top right of the anchor. The melting of ice crystals in the soil body into pore water caused the volume of the liquid phase to shrink, but the spacing of the soil particles could not shrink. Frozen expansion caused cracks inside the soil body, which collapsed under self-weight stress. However, the part of the soil that froze and swelled

adsorbed a large amount of water from the surrounding area in the process of freezing and had a large water content after thawing, which caused drainage consolidation and settlement under the action of self-weight stress; the stability and integrity of the anchored soil was damaged. A schematic diagram of water migration during freeze–thaw cycles is shown in Figure 18.

(2) The effect of freeze–thaw damage increased significantly with increasing moisture content. The thawing and sinking resistance for 10, 12 and 14% water content conditions were 71, 68 and 52% of that before freezing, respectively. Water migration and swelling during freezing and thawing became more significant at greater water content, causing more loosening of soil particles and more severe loss of shear capacity at the anchor–soil interface.



(**a**) Freezing process (**b**) Melting process

Figure 18. Schematic diagram of freeze–thaw moisture migration.

4. Discussion and Conclusions

In this study, we conducted indoor pull-out model tests on anchor rods with different moisture contents and freezing temperatures, quantitatively described the changes in anchor rod pull-out force before and after freezing, plotted load–displacement curves, observed and recorded the freezing displacement of the anchor rod and stress evolution of the surrounding soil under asymmetric negative temperature loading, and reached the following main conclusions:

(1) The pull-out force of the anchor increased with increasing axial displacement, and the change process was divided into three stages: "fast growth", "slow growth" and "constant growth". The pull-out force increased with increasing anchorage diameter, and the pull-out forces for 35 and 40 mm diameters were 1.102 and 1.306, 1.089 and 1.254, and 1.091 and 1.248 times that of 30 mm for the three water content conditions, respectively. The shear strength and pull-out force at the anchor interface decreased with increasing water content. When the water content increased from 10 to 12 and 14% for 30 mm diameter anchorages, the anchor pull-out force decreased by 0.039 and 0.064 kN, or 7.96% and 13.1%, respectively.

(2) The test soil entered the frozen state by the negative temperature load, and the frozen area continued spreading from the cold source at the upper right through the whole soil specimen with increased freezing time. The anchor rods were in an asymmetric stress state for a long time due to the influence of the single-side freezing method, and they were displaced under the action of the freezing expansion force. Taking the moisture content of 10% as an example, the lateral displacements of anchors at 0, −3 and −7 °C were 2.9, 3.2 and 3.5 mm, and the vertical displacements were 0.2, 3.5 and 4.3 mm, respectively. The total displacement increased with increasing moisture content; the maximum horizontal displacements were 3.5, 3.65 and 3.8 mm under 10,

12 and 14% moisture content working conditions, and the vertical displacements were 4.3, 5.1 and 5.5 mm, respectively.

(3) The shear strength of the anchor–soil interface increased as the temperature decreased, and the ultimate value of the pull-out force increased as the temperature decreased and the moisture content increased. The pull-out force of the frozen anchor increased with increasing water content.

(4) After freezing and thawing. the ultimate pull-out forces were 71, 68 and 52% of that before freezing under 10, 12 and 14% moisture content working conditions, respectively.

Author Contributions: Conceptualization, J.D.; Methodology, J.D.; Validation, X.Y. and Z.-Q.L.; Formal analysis, J.D., X.Y. and Z.-Q.L.; Investigation, X.Y.; Resources, J.D. and Y.-H.Z.; Data curation, J.D., X.Y., Z.-Q.L. and Y.L.; Writing—original draft, X.Y.; Writing—review & editing, K.F.; Visualization, Y.-H.Z.; Supervision, Y.L., Y.-H.Z. and K.F.; Project administration, Y.L.; Funding acquisition, J.D. All authors have read and agreed to the published version of the manuscript.

Funding: The research described in this paper was financially supported by the Natural Science Foundation of China (NO. 51878242), the Natural Science Foundation of Hebei Province of China (NO. E2020404007), the Doctoral Research Start-up Fund Project (B-202101), the Research Project of Basic Scientific Research Business Fund for Higher Education Institutions in Hebei Province (2021QNJS07), the Research Project on Basic Research Funds for Higher Education Institutions in Hebei Province (2021QNJS02), Hebei Provincial Department of Education Innovative Ability Training Program for graduate students (CXZZSS2022063).

Institutional Review Board Statement: Not applicable.

Informed Consent Statement: Not applicable.

Data Availability Statement: Data will be made available on request.

Conflicts of Interest: The authors declare no conflict of interest.

References

1. Kang, H.P.; Lin, J.; Fan, M.J. Investigation on support pattern of a coal mine roadway within soft rocks—A case study. *Int. J. Coal Geol.* **2015**, *140*, 31–40. [CrossRef]
2. Jeong, Y.Y.; Kang, H.M.; Choi, S.H.; Cho, S.H. Dynamic expansion rock bolt for rapid installing in rocks. *Geosystem Eng.* **2015**, *18*, 85–91. [CrossRef]
3. Shi, Z.M.; Liu, L.; Peng, M.; Liu, C.C.; Tao, F.J.; Liu, C.S. Non-destructive testing of full-length bonded rock bolts based on HHT signal analysis. *J. Appl. Geophys.* **2018**, *151*, 47–65. [CrossRef]
4. Zhou, Y.D.; Cheuk, C.Y.; Tham, L.G. Numerical modelling of soil nails in loose fill slope under surcharge loading. *Comput. Geotech.* **2009**, *36*, 837–850. [CrossRef]
5. Cui, Y.H.; Liu, J.K.; Lv, P. Development of a dynamic load direct shear apparatus for the study of permafrost. *Sci. Cold Arid Reg.* **2013**, *5*, 399–403. [CrossRef]
6. Zhao, L.-Z.; Yang, P.; Wang, H.-B. Development and application of large-scale multi-functional frozen soil-structure interface cycle-shearing system. *Dam Saf.* **2013**, *35*, 707–713.
7. Cui, Y.H.; Liu, J.K.; Lv, P. Research of the permafrost dynamic load direct shear apparatus. *Appl. Mech. Mater.* **2013**, *405*, 454–459. [CrossRef]
8. Lv, P.; Liu, J.; Cui, Y. A study of dynamic shear strength of frozen soil-concrete contact interface. *Rock Soil Mech.* **2013**, *34*, 180–183.
9. Gao, Q.; Wen, Z.; Wang, D.; Niu, F.; Xie, Y.; Gou, T. Study on the instability process of slopes in permafrost regions by direct shear test of freezing-thawing interface. *Rock Soil Mech.* **2018**, *39*, 2814–2822.
10. Xu, X.-Z.; Wang, J.-C.; Zhang, L.X. *Physics of Permafrost*; Science Press: Beijing, China, 2010; pp. 198–205.
11. Ma, W.; Wang, D.-Y. *Mechanics of Frozen Ground*; Science Press: Beijing, China, 2014; pp. 39–95.
12. Shen, Y.-P. *Study of Stability of Embankment upon the Slope in the Permafrost Area at Anduo Section of Qinghai-Tibet Railway*; Beijing Jiaotong University: Beijing, China, 2007.
13. Wen, Z.; Yu, Q.H.; Ma, W.; Dong, S.; Niu, F.; Wang, D.; Yang, Z. Direct shear teats for mechanical characteristics of interface between Qinghai-Tibetan silt and fiberglass reinforced plastics. *Rock Soil Mech.* **2013**, *34* (Suppl. 2), 45–50.
14. Zhang, D.-J.; Lu, T.-H. Establishment and application of a interface model between soil and structure. *Chin. J. Geotech. Eng.* **1998**, *20*, 65–69.
15. Chen, W.H. Experimental Research on Frozen Strength and Negative Friction of Pile Side in Permafrost Regions. Ph.D. Thesis, Harbin Institute of Technology, Harbin, China, 2011.

16. Li, H.; Zhu, Y.; Zhang, J.; Lin, C. Effects of temperature, strain rate and dry density on compressive strength of saturated frozen clay. *Cold Reg. Sci. Technol.* **2004**, *39*, 39–45. [CrossRef]
17. Liu, J.; Lv, P.; Cui, Y.; Liu, J. Experimental study on direct shear behavior of frozen soil–concrete interface. *Cold Reg. Sci. Technol.* **2014**, *104–105*, 1–6. [CrossRef]
18. Xu, X.; Wang, Y.; Yin, Z.; Zhang, H. Effect of temperature and strain rate on mechanical characteristics and constitutive model of frozen helin loess. *Cold Reg. Sci. Technol.* **2017**, *136*, 44–51. [CrossRef]
19. Andersland, O.B.; Ladanyi, B. *Frozen Ground Engineering*; John Wiley & Sons: Hoboken, NJ, USA, 2003.
20. Jones, S.J. The confined compressive strength of polycrystalline ice. *J. Glaciol.* **2017**, *28*, 171–178. [CrossRef]
21. Yang, Z.; Still, B.; Ge, X. Mechanical properties of seasonally frozen and permafrost soils at high strain rate. *Cold Reg. Sci. Technol.* **2015**, *113*, 12–19. [CrossRef]
22. Wen, Z.; Yu, Q.; Ma, W.; Dong, S.; Wang, D.; Niu, F.; Zhang, M. Experimental investigation on the effect of fiberglass reinforced plastic cover on adfreeze bond strength. *Cold Reg. Sci. Technol.* **2016**, *131*, 108–115. [CrossRef]
23. Aldaeef, A.A.; Rayhani, M.T. Pile-soil interface characteristics in ice-poor frozen ground under varying exposure temperature. *Cold Reg. Sci. Technol.* **2021**, *191*, 103377. [CrossRef]
24. Aldaeef, A.A.; Rayhani, M.T. Adfreeze strength and creep behavior of pile foundations in warming permafrost. In *Advances in Analysis and Design of Deep Foundations*; Abu-Farsakh, M., Alshibli, K., Puppala, A., Eds.; Springer International Publishing: Cham, Switzerland, 2018; pp. 254–264.
25. Aldaeef, A.A.; Rayhani, M.T. Impact of ground warming on pile-soil interface strength in ice-poor frozen soils. In Proceedings of the GeoEdmonton 2018 Conference, Canadian Geotechnical Society, Edmonton, AB, Canada, 23–26 September 2018.
26. Aldaeef, A.A.; Rayhani, M.T. Influence of exposure temperature on shaft capacity of steel piles in ice-poor and ice-rich frozen soils. In *Sustainability Issues for the Deep Foundations*; El-Naggar, H., Abdel-Rahman, K., Fellenius, B., Shehata, H., Eds.; Springer International Publishing: Cham, Switzerland, 2019; pp. 247–257.
27. Aldaeef, A.A.; Rayhani, M.T. Load transfer and creep behavior of open-ended pipe piles in frozen and unfrozen ground. *Innov. Infrastruct. Solut.* **2019**, *4*, 60. [CrossRef]
28. Wang, J.; Nishimura, S.; Tokoro, T. Laboratory study and interpretation of mechanical behavior of frozen clay through state concept. *Soils Found.* **2017**, *57*, 194–210. [CrossRef]
29. Kingsbury, D.W.; Sandford, T.C.; Humphrey, D.N. Soil nail forces caused by frost. *Transp. Res. Rec.* **2002**, *1808*, 38–46. [CrossRef]
30. Stocker, M.F.; Riedinger, G. The bearing behaviour of nailed retaining structures. In *Design and Performance of Earth Retaining Structures*; ASCE: Reston, VA, USA, 1990; pp. 612–628.
31. Johnston, G.H.; Ladanyi, B. Field tests of deep power-installed screw anchors in permafrost. *Can. Geotech. J.* **1974**, *11*, 348–358. [CrossRef]
32. Aldaeef, A.A.; Rayhani, M.T. Pull-out capacity and creep behavior of helical piles in frozen ground. *J. Geotech. Geoenvironmental. Eng.* **2020**, *146*, 04020140. [CrossRef]
33. Zhang, Y.; Dong, J.H.; Dong, X.G.; Wang, Y.S. Analysis of freezing and thawing of slope improved by soil nailing structure in seasonal frozen soil region. *Rock Soil Mech.* **2017**, *38*, 574–582. [CrossRef]
34. Wu, Z.-W. Groundwater characteristics of permafrost layer along Qinghai-Tibet highway. In *The 50 Years of Permafrost Research—The Corpus of Wu, Z.-W., Zhou, Y.-W.*; Science Press: Beijing, China, 2010; pp. 180–190.
35. Zhao, G.; Tao, X.-X.; Liu, B. Experimental study on water migration in undisturbed soil during freezing and thawing process. *Chin. J. Geotech. Eng.* **2009**, *31*, 1952–1957.
36. Zhang, W.; Wang, L.; Song, Y.; Tan, Y. Experimental study on the mechanical properties of grouted rock bolts subjected to sulfate attack and freeze-thaw cycling. *Constr. Build. Mater.* **2021**, *291*, 123391. [CrossRef]

Disclaimer/Publisher's Note: The statements, opinions and data contained in all publications are solely those of the individual author(s) and contributor(s) and not of MDPI and/or the editor(s). MDPI and/or the editor(s) disclaim responsibility for any injury to people or property resulting from any ideas, methods, instructions or products referred to in the content.